International Journal of Social Robotics
https://doi.org/10.1007/s12369-025-01216-7

Enhancing Object Release Fluency in Robot to Human Handover Using Proprioceptive and Exteroceptive Information

Mattia Penzotti[1,2] · **Marco Controzzi**[1,2]

Accepted: 16 January 2025

Abstract
Object handover is the fundamental collaborative action requiring robots and humans to physically interact. When the robotic partner plays the giver role, it assumes the responsibility of safely and fluently conducting the handover, aiming to enhance the quality of the action perceived by the human receiver. In these terms, complex scenarios, such as conditions for which the robot must reach the partner to present the object to handover, really pose the challenge of preserving good coordination concerning the observed intention of the human. A crucial aspect is gaining the correct timing for the beginning of the object release and controlling its duration. Here we show that robot proprioception and observation of the human partner kinematics are key aspects to successfully deal with these issues. We present a handover control policy based on two modules. The first consists of a filtering technique which guarantees the correct reactivity of the robot by estimating and interpreting the interaction forces generated during the handover. The second module is a bio-inspired control law for the object release, aiming for the best possible coordination with the human partner. The control policy has been implemented in a robot arm equipped with a sensorised artificial hand and assessed by 15 participants asked to hand over a test object using different reaching dynamics. The control policy proved to be reliable since we did not record failures of the handover in 180 trials, and coordinated to the handover dynamics of the receiver, although it did not outperform fast feed-forward releases.

Keywords Handover · Human-robot interaction · Proprioception

1 Introduction

Despite the recent advances in AI to potentially allow robots to carry out tasks without any human intervention [1], the full autonomy of robots is still a chimera [2]. In industrial environments, there are many applications requiring robots to be supervised or work alongside humans. Pick and place, packaging and palletizing, machine tending, and quality inspection are four of the main applications for cobot deployments. In these applications, robots can handle repetitive tasks without distraction, tiredness, and boredom. The collaboration with humans enables adaptability towards unforeseen changes in the environment that would impede the robot from accomplishing the task [3]. At home, robots able to safely interact with humans can improve the independence and quality of life of persons with disabilities, providing physical assistance during the day [4].

A great research effort has been made to empower robots with physical interaction abilities [3, 5, 6]. One of these is the object handover [7], since it represents the most basic, yet fundamental, collaborative action. Object handover is a joint action which involves one agent, a passer, transferring an object to a partner, or receiver. Even if humans accomplish it without effort, object handover requires efforts in prediction, perception, and adjustment to others. This is the reason why the implementation of a seamless robot-to-human handover is even today an ambitious challenge. The handover is composed of the succession of two phases [8]: pre-handover and physical handover. The first includes all the preparatory actions the two agents perform before the first contact between the receiver's hand and the object [9]. The latter is the action beginning with the contact of the receiver's hand

✉ Marco Controzzi
marco.controzzi@santannapisa.it

Mattia Penzotti
mattia.penzotti@santannapisa.it

[1] The Biorobotics Institute, Scuola Superiore Sant'Anna, Viale Rinaldo Piaggio 34, 56025 Pontedera, Pisa, Italy

[2] Department of Excellence in Robotics and AI, Scuola Superiore Sant'Anna, Piazza Martiri della Libertà 33, 56127 Pisa, Italy

Published online: 13 February 2025

on the object held by the giver and is strongly related to the grip force modulation of the two agents [10]. The pre-handover phase has been widely investigated in robotics, mostly focused on the generation of safe and legible reaching trajectories [11–16], grasp actions [17] or non-verbal cues to suggest the handover location [18] or the correct timing [19]. However, the grip force modulation of the giver plays an important role in producing a seamless interaction with the receiver [8, 20, 21]. A key aspect is the way humans rely on visual input, to properly trigger the object release, by anticipating and predicting the beginning of the corresponding physical handover phase [10]. The anticipatory behaviour is considered a response to the latency affecting pure somatosensory feedback in humans, as quantified by the analysis of handover behaviour in blindfolded participants in [10]. Thanks to the extremely high control frequency of the hardware equipping a robot co-worker, playing the role of the giver, this latency is negligible, and the predominance of exteroceptive information (i.e., sensors measuring the forces generated by an interaction with an external agent or the environment) can be assumed more than sufficient for the overall quality of the collaborative action [22]. We also proved that a human giver, adjusts the release duration, according to the observed receiver's peak acceleration. In particular, the faster the reaching motion of the receiver, the faster the object is released by the giver [10]. In the present work, we want also to experimentally investigate the benefits given by implementing a similar bio-inspired control strategy in a robotic giver. According to exteroceptive information, different methods have been proposed to manage uncertain events occurring in the case of a static handover [23], while a comparatively small amount of previous literature has explored the dynamic scenario [24]. In the present work, we address the problem of an optimal and reliable transition between the pre-handover and the physical handover phase, considering the case of a human receiver that grasps the object while the robotic giver is still moving toward the handover location. If the human worker is confident about the robot's behaviour, she/he can coordinate her/his action with the movement of the robotic arm, thus contacting the object before the arm completely stops. In this case, gaining proper timing in the object release can be challenging. Indeed, the sensor signals of the robot comprise proprioceptive (i.e., forces generated by the motion of the body/robot) and exteroceptive (e.g., mild collision with the receiver) information. Thus, because of the unknown inertia of the grasped object, while reaching the handover position, the receiver may not be precisely detected by the force/torque sensors of the robot, leading to a delayed object release.

Here we present a proprioceptive filtering technique which indeed requires an online object recognition (i.e., an estimate of the object inertial parameters) after the grasp action and thus before handing it over to the human receiver. The information to filter is assumed to be provided from a force/torque sensor interposed in between the robot mounting plate and the end effector (i.e., any kind of gripper) and is based on [25]. To assess the functionality of the proposed technique, participants are asked to complete an experimental session acting as receivers, while a collaborative robot plays the role of the giver in the scenario of robot-to-human object handover. In section 2 the mathematical framework for proprioceptive filtering along with a method to optimise the required estimation process are presented, in section 3 the experimental setup is described, comprising of used hardware and control strategies. In section 4 experimental protocol and results are presented, along with discussion and conclusion in section 5.

2 Methods

2.1 Proprioceptive Filtering

Referring to the notation proposed in [25], we consider ${}^{\mathbf{S}}\phi_{10\times1}$ the complete set of inertial parameters to be estimated. Since the proprioceptive information is related to the sensor measurement frame $\mathbf{S}$, the applied force and torque vectors, combined in the compact notation ${}^{\mathbf{S}}\mathbf{f}_{6\times1}$, are related to the frame kinematics through the Newton-Euler equations, in particular, the coefficients matrix $\mathbf{V}_{6\times10}$ leads to the compact formula:

$$ {}^{\mathbf{S}}\mathbf{f} = \mathbf{V}\,{}^{\mathbf{S}}\phi \tag{1} $$

This relationship is valid for any instant of time, hence assuming to collect the left member of Eq. (1) plus the related $\mathbf{V}$ matrix in N time steps (for instance sampling the state of the system during an ad-hoc trajectory, as depicted in the next section), it follows the linear system of equations:

$$ \mathbf{f}^* = \left[{}^{\mathbf{S}}f_1^\top, \ldots, {}^{\mathbf{S}}f_N^\top\right] \tag{2} $$

$$ \mathbf{V}^* = \left[{}^{\mathbf{S}}V_1^\top, \ldots, {}^{\mathbf{S}}V_N^\top\right] \tag{3} $$

$$ \mathbf{f}^* = \mathbf{V}^* \left[{}^{\mathbf{S}}\phi_1^\top, \ldots, {}^{\mathbf{S}}\phi_N^\top\right]^\top \tag{4} $$

By assuming that all the N inertial sets collected by the vector on the right hand of Eq. (4) are identical to each other. This means considering that no elasticity exists in the mechanical system attached to the force/torque sensor and that the object cannot move with respect to the gripper frame (i.e., no relative displacement occurs, due to a not perfectly stable grasp). Moreover, this assumption leads to solving Eq. (4) with respect to ${}^{\mathbf{S}}\phi$ as a nonlinear least squares problem. By using a Levenberg-Marquardt optimiser, mass and diagonal elements of the inertia tensor are constrained to be positive. Once an optimised set for ${}^{\mathbf{S}}\phi$ is known, from the kinematic state $\mathbf{V}_i$ in the generic i^{th} time step, Eq. (1) gives an estimate

of applied force/torque vector ${}^{\mathbf{S}}\mathbf{f}_{pr}$ (the pr subscript indicates a proprioceptive information). The expected result of filtering the proprioceptive information is then produced by the subtraction of these quantities from ${}^{\mathbf{S}}\mathbf{f}$ (i.e., actual sensor readings), hence:

$$ {}^{\mathbf{S}}\mathbf{f}_e = {}^{\mathbf{S}}\mathbf{f} - {}^{\mathbf{S}}\mathbf{f}_{pr} \tag{5} $$

where the e subscript indicates exteroceptive information. To fill the $\mathbf{V}_i$ matrix, the complete joint states must be known for the considered kinematic chain, going from the manipulator reference frame **B** to **S**. Collecting the joint angles vector $\mathbf{q}$ and the joint velocities $\dot{\mathbf{q}}$ from the real hardware, the joint accelerations $\ddot{\mathbf{q}}$ can be obtained by numerical differentiation of $\dot{\mathbf{q}}$. The joint angles vector q also leads to the composition of the global rotation matrix $\mathbf{R_{BS}}$ from **B** to **S**. Making use of the geometric Jacobian $\mathbf{J}(\mathbf{q})$ it follows:

$$ \left[{}^{\mathbf{S}}\mathbf{v}^{\top}, {}^{\mathbf{S}}\omega^{\top}\right]^{\top} = \mathbf{R_{BS}}\mathbf{J}(\mathbf{q})\,\dot{\mathbf{q}} \tag{6} $$

$$ \left[{}^{\mathbf{S}}\mathbf{a}^{\top}, {}^{\mathbf{S}}\alpha^{\top}\right]^{\top} = \mathbf{R_{BS}}\left(\mathbf{J}(\mathbf{q})\,\ddot{\mathbf{q}} + \dot{\mathbf{J}}(\mathbf{q}, \dot{\mathbf{q}})\,\dot{\mathbf{q}}\right) \tag{7} $$

Considering the sensor frame twist, $\mathbf{v}$ and $\boldsymbol{\omega}$ represent its linear and angular components, respectively. Similarly, $\mathbf{a}$ and $\boldsymbol{\alpha}$ denote the frame's linear and angular acceleration components. Please find in [26] details on the computation of Jacobian time derivative $\mathrm{J}'\left(\mathrm{q}, \mathrm{q}'\right)$ in hybrid representation.

2.2 Estimation Trajectory Optimisation

We want to optimise the trajectory to perform the estimation of the inertial set, representing the attached gripper and the grasped object. The scope of this optimisation is reducing the effect of the measurement noise affecting the joint state readings and the force/torque sensor, which is found to be much higher as the condition number $\kappa(\mathbf{V}^*)$ grows. The singular values of a matrix $\mathbf{X}$ are the square root of the n eigenvalues of $\mathbf{X}^{\top}\mathbf{X}$, the condition number of $\mathbf{X}$ is defined as the ratio between the largest and smallest of its singular values. Considering **S** to be also the controlled frame in the estimation trajectory, each Degree of Freedom (DOF) is constrained to follow an instantaneous time variation rate ${}^{S}\dot{y}(t)$ given by the composition of harmonics [27] in the form:

$$ {}^{S}\dot{y}_i = \sum_{j=1}^{N_i} h_i\,(j T_S)^{-1}\left(1 - \cos 2\pi\, j T_s^{-1}\right) \tag{8} $$

where i represents the generic DOF expressed with respect to the instantaneous frame **S** (translational or rotational in XYZ Euler angles notation). N_i is the total number of harmonics to compose, h_i is the fundamental amplitude and T_s is the trajectory goal time. Please note that T_s is constant (not parameterised with respect to i) and that the amplitude of each harmonic is scaled down by the order j, thus limiting the growth of displacement along the generic DOF for an increasing number of contributing terms.

We modelled the kinematics of a UR5 CB3 6-DOFs robot arm (Universal Robots A/S) in the MATLAB® Robotics System Toolbox™, where inputs to the Inverse Kinematics (IK) solver (embedded in the toolbox) are provided by imposing to S displacements given by one step of Euler integration of Eq. (8) and applied to its instantaneous configuration. A total number of 16 hyper-parameters are then selected for Bayesian optimisation of $\kappa(\mathbf{V}^*)$. Along with $N_i \in [0, 4]$ and $T_s \in [0.5, 3]$, a normalised amplitude $h_i^* \in [-1.0, 1.0]$ is considered for each DOF, then a global scaling factor $h_g \in [0.1, 0.5]$ is introduced in the optimisation process. To also consider the effect of the initial orientation of **S** with respect to gravity, we include the $y_0 \in [0, \pi]$ and $z_0 \in [-\pi, \pi]$ angles. Assuming that the z-axis of the measurement frame is aligned against the gravity vector for $y_0 = 0$ and $z_0 = 0$, a rotation on the y-axis of y_0 combined with a further rotation on the z-axis of the rotated frame by z_0, produces the desired effect to allow any initial orientation of the measurement frame with respect to gravity. The h_g parameter uniformly scales the fundamental displacement on each DOF. Trajectories causing singular configurations and excessive accelerations at the joint level are considered unfeasible. To evaluate $\kappa(\mathbf{V}^*)$ also considering noise in joint angle measurements, at each time step $t_i \in [0, T_s]$, the joint set $\mathbf{q}_i$ from the IK solver is summed to a blank noise vector before computation of Forward Kinematics. For each i^{th} time step, such a vector randomly samples n Gaussian distributions, with standard deviation σ_n derived by observing the noise affecting the n^{th} joint angle readings in the real system. After 20 iterations of the `bayesopt` function from the MATLAB®Optimisation Toolbox™, each of them limited to a maximum of 200 objective evaluations, the optimal set of hyper-parameters which minimises $\kappa(\mathbf{V}^*)$ is selected.

3 Setup

3.1 Hardware

To quantify the benefits given by proprioceptive filtering in the handover scenario, we use the ROS framework to integrate and control the required hardware. The robotic platform comprises a UR5 CB3 6-DOFs robot arm (Universal Robots A/S), equipped with a HEX-E V2 6-axis force/torque sensor (OnRobot A/S) and a Mia Hand gripper (Prensilia s.r.l.) with built-in finger 2-axis strain sensors (index, medium and thumb). The test object is a lightweight prism (mass less than 100 g) and sides 50 × 50 × 150 mm. On the affordance of the object which is presented by the robot to participants for

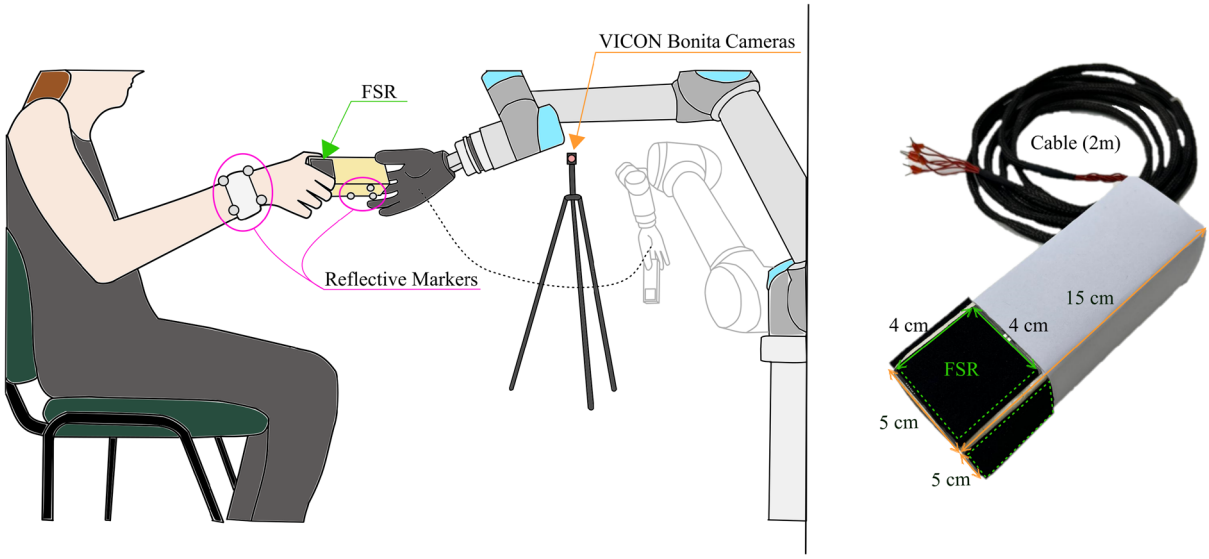

Fig. 1 On the left side, the experimental setup. The participant sits in front of the robot arm. The robot initiates the execution of the handover by grasping the target object on the desk and then handing over the object to the human. The kinematics of his/her right hand and of the object are tracked using a motion capture system. On the right, the object used for the experiment, which has been equipped with Force Sensing Resistors to measure the contact of the receiver

the handover, we placed 4 square Force Sensing Resistors (FSR), one for each longitudinal surface of the prism, of size 40 mm. We use the analog inputs of the UR5 control box to acquire the FSR signals. The strain resistors are connected two by two in a parallel configuration, each tuple of sensors is attached to the test object so that they lie on adjacent surfaces, thus a secure grasp on the sensorised affordance causes the activation of both circuits. The kinematic state of the participants' right hand is tracked using a motion capture system comprising 6 infrared Bonita cameras (Vicon Ltd.) and the proprietary motion capture software Nexus (Vicon Ltd.), which runs on a dedicated working station. A synthetic representation of the final setup is depicted in Fig. 1.

3.2 Control Frequencies

The sampling frequency is set to 500 Hz for the force/torque sensor and 125 Hz for the joint angles and joint velocities measured by the robotic arm (the same applies to the analogic state of FSR sensors), while the coefficients of $\mathbf{V}_i$ are obtained for the i^{th} time step according to a loop rate of 50 Hz for the composition of $\mathbf{V}^*$, consequently the same rate is applied to the composition of $\mathbf{f}^*$, for further estimation of the inertial set ${}^{\mathbf{S}}\phi$ and for the actual proprioceptive filtering during the reaching phase. The Mia Hand sampling frequency and control loop are fixed at the maximum rate of 20 Hz. Data from the Vicon motion capture system stream into the ROS framework at 120 Hz. Concerning the motion capture data, we apply a cascade of two 8 samples Savitzky-Golay filters to estimate linear velocities and accelerations from the time-varying position of any tracked rigid body.

3.3 Trajectory Control

For the reaching phase and as well for any other point-to-point motion performed by the manipulator (thus except during the estimate of inertial parameters), minimum-jerk trajectories are generated to control the maximum linear/angular accelerations and to achieve smoothness. We define $h = \max\left(\mathbf{x}_0 - \mathbf{x}_f\right)$ where $\mathbf{x}_0$ and $\mathbf{x}_f$ are the initial and target position of the end-effector. In general, we define $\ddot{\mathbf{x}}(t)$ as the second time-derivative of $\mathbf{x}(t)$, and giving that:

$$\ddot{x}_{\max}(h) = c_a h T_a^{-2} \tag{9}$$

setting the acceleration limit $\ddot{x}_{\max}$ and since $c_a = 5.8$ (for minimum-jerk trajectory) we can obtain the desired completion time T_a. Similarly, one can limit the angular acceleration by setting $h = \theta$, where θ is the angular displacement about the rotation axis (axis-angle notation). Thus, time-varying target position and orientation along with the desired end-effector twist are the inputs for a first-order closed-loop IK algorithm based on the Jacobian pseudo-inverse. Desired joint velocities are then forwarded to the manipulator through the velocity interface via the official Universal Robots ROS driver.

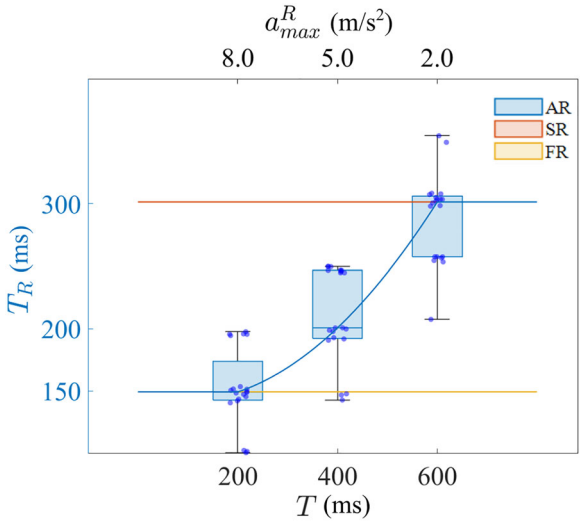

Fig. 2 Experimental characterisation of T_R as a function of T and proposed Adaptive Release (AR) control law correlating $a^R_{\max}$ to T_R (and thus to T). Extreme T_R values of AR are used for fixed Slow Release (SR) and Fast Release (FR) laws

3.4 Release Control

We assumed that the inertial estimation process has been performed before the reaching phase. At the very beginning of this phase, the proprioceptive filtering algorithm is applied to produce the exteroceptive quantities ${}^{\mathbf{S}}\mathbf{f}_e$. Given d_{thre} the distance threshold from the receiver's hand (tracked for instance by the motion capture system) and the manipulator end-effector, depending on the actual giver/receiver distance d, we define:

$$\begin{cases} {}^{\mathbf{S}}\mathbf{f}_{thre,j} = \max\left({}^{\mathbf{S}}\mathbf{f}_{thre,j}, {}^{\mathbf{S}}\mathbf{f}_{e,j}\right) \\ \quad r_{a,j} = 0 \end{cases} \quad \text{if} \quad d > d_{thre}$$

$$r_{a,j} = {}^{\mathbf{S}}\mathbf{f}_{thre,j} < 1.5\,{}^{\mathbf{S}}\mathbf{f}_{e,j} \quad \text{if} \quad d \leq d_{thre}$$

for $j \in [1, 6]$. The release activation occurs if $r_a > 0$, thus if the robotic giver is closer to the receiver than a fixed distance, it will begin to release the object whenever any of the j^{th} estimated exteroceptive force/torque components overcomes by 50 per cent the stored threshold ($thre$ subscript). For the experimental session, d_{thre} is fixed to 50 cm. To gently stop the arm motion on release activation, the time-varying velocity given by the minimum-jerk trajectory is smoothly scaled down through a modified Hanning function, with time span (i.e., stop time) of 0.5 s, in this case, the desired end-effector position is replaced by the Euler integration of the scaled twist.

To further control the object release we use stereotypical synchronous joint trajectories for the Mia hand. Giving that $\mathbf{x_0}$ is the vector of the initial joint angles of the Mia hand 3-DOFs gripper holding the test object, and $\mathbf{x_f}$ is the desired final (open) configuration, we apply the control law:

$$\dot{\mathbf{x}}(t) = T^{-1}\left(\mathbf{x}_f - \mathbf{x}_0\right)\left(1 - \cos\left(2\pi t T^{-1}\right)\right) \tag{10}$$

where T is the completion time. The velocity command for each joint for the generic time step is then forwarded to the Mia Hand via the official ROS driver. The release time T_R does not in general match with the completion time T, for this reason, we experimentally characterised T_R as a function of T, keeping fixed the grasp configuration on the test object, in terms of contact points and applied force. While releasing the object (hence the hand opens), we identify T_R as the duration from the beginning of fingers motion (i.e., any of the motor encoders measures speed different than zero) to the loss of contact force of the fingers with the test object (i.e., any of the embedded strain gauge sensor readings falls under 20 g) [28]. According to empirical results, we also define an adaptive release control law, as in Fig. 2, which correlates the observed maximum value of the receiver's acceleration magnitude $a^R_{\max}$ (while reaching the object) to the desired T_R.

4 Experimental Protocol

The participant sits in front of the robotic arm and outside of its workspace, configured through safety features (planes) as by the Universal Robots user manual. Thus it is guaranteed, for safety reasons, that a physical interaction between receiver (participant) and giver (robotic arm), may occur only if the receiver extends his arm toward the robot workspace, aiming to complete the object handover. The spatial pose of the test object with respect to the robot base is retrieved as needed via the motion capture system, hence the manipulator can repeatably and autonomously grasp the object.

For each participant, the experimental session did not last longer than 40 min and can be divided into three main steps. The first one is the calibration phase, where we calibrate the motion capture cameras, both in terms of their relative pose (via Nexus) and in terms of merging the motion capture reference frame with the robot base (via ROS). We then calibrated the force/torque sensor to get rid of any thermal drift and mounting offsets and finally, we performed the estimation trajectory and stored the resulting inertial set. Since the robot grasps the same test object autonomously, as well in the calibration phase as in the further phases, we need to perform the estimation once per participant (i.e., every time a new calibration is performed).

The second step is a familiarisation phase, where participants observed at least once the full-reaching trajectory performed by the manipulator. In the reaching phase for the object handover, the target pose is chosen such that the position is frontal with respect to the receiver and lying

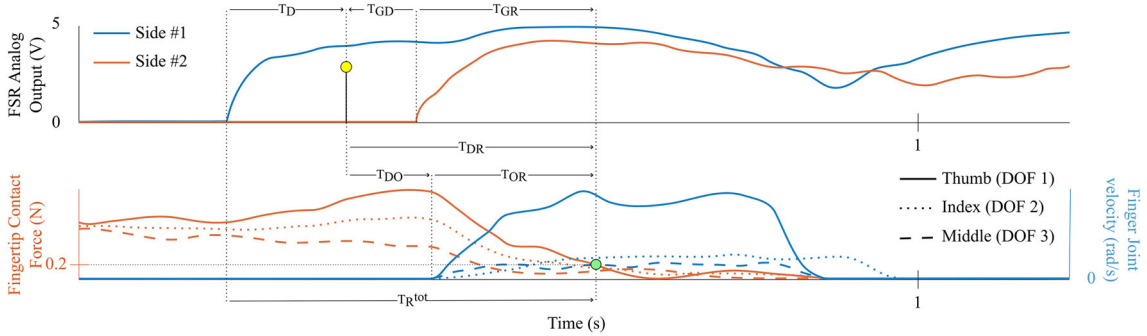

Fig. 3 On the top graph it is displayed the output of the sensorised object. The yellow dot indicates the beginning of the object release procedure. On the bottom graph it is displayed the contact force measured at the fingertips of the hand, overlayed to fingers joint velocities. The green dot signals the end of the physical handover (i.e., contact forces lower than minimum contact threshold, see Sect. 3.4)

in a parasagittal plane passing through his right shoulder, with respect to the shoulder, the height is slightly lower and the distance is ∼40 cm. The orientation, according to the grasp configuration, is taken to present the test object with its longest axis perpendicular to the frontal plane of the receiver so that the sensorised affordance is clearly accessible to her/him. Participants are asked to contact the test object before the arm completely stops, trying to begin the physical phase of the handover as soon as they can reach the object, and secure their grasp on the sensorised surface. They are also asked to regulate their reaching speed with respect to the behaviour assumed by the robot, for which we fixed two levels of reaching dynamics, characterised respectively by a peak acceleration for the minimum-jerk trajectory of 1.0 m/s^2 for the Low Speed (LS) reaching and 2.0 m/s^2 for the High Speed (HS) reaching. In the first case, participants should learn to exhibit peak acceleration lower than 3.0 m/s^2, greater than 4.0 m/s^2 in the second case.

The third step is the actual experimental phase, where a total of 36 valid (satisfying all the constraints required of participants) repetitions are performed. If the trial is not valid, it is discarded and repeated. The total number of 36 is subdivided into 6 subsequent blocks of experimental conditions, given from the combination of the two levels of timing (LS and HS) and of three types of release behaviour that the gripper may assume. The first one is an Adaptive Release (AR), where the release speed is regulated by the control law depicted in Sect. 3, then also a fixed Slow Release (SR) and fixed Fast Release (FR) are included, where the release duration is respectively the maximum or the minimum that the adaptive control law may assume.

4.1 Output Metrics

As subjective metrics, for each valid repetition, participants are asked to rate the handover fluency on a 7-point scale, ranging from −3 to +3. Participants are asked to rate the interaction with negative values whenever the robotic agent is perceived as being delayed in the physical handover phase, for instance starting too late to release the object. On the contrary, positive values have the meaning of rating the robotic agent as being early in the physical handover phase, for instance releasing the object too fast according to the participant's experience of the interaction. The null value indicates a neutral condition for which the participant does not perceive any coordination issue while receiving the object in the physical handover phase.

The objective metrics, qualitatively depicted in Fig. 3 are:

- Time to detection T_D, as the time elapsed from the instant of the first activation of one of the two FSR circuits (very first contact of the receiver's hand with the object) to the signalling of the object release. It measures the effectiveness of proprioceptive filtering in achieving early detection of the beginning of the physical handover phase;
- Time from detection to release T_{DR}, as the time elapsed from the signalling of the object release, to the end of the object release. It measures the total duration of the object release procedure implemented on the robotic agent, starting from the very beginning of the physical handover phase;
- Time from detection to open T_{DO}, as the time elapsed from the signalling of the object release to its actual beginning (i.e., any of the Mia hand motor encoders measures speed different than zero). It measures the actuation delay on the robotic agent due to system communication latencies;
- Time from open to release T_{OR} (i.e., time to release T_R, see Sect. 3) as the time elapsed from the very beginning of the object release to the loss of contact force of the Mia hand fingers with the test object. It measures the effective object release duration to be compared to timings observed in human-to-human handovers;
- Time from grasp to detection T_{GD}, as the time elapsed from the instant of the first activation of both FSR cir-

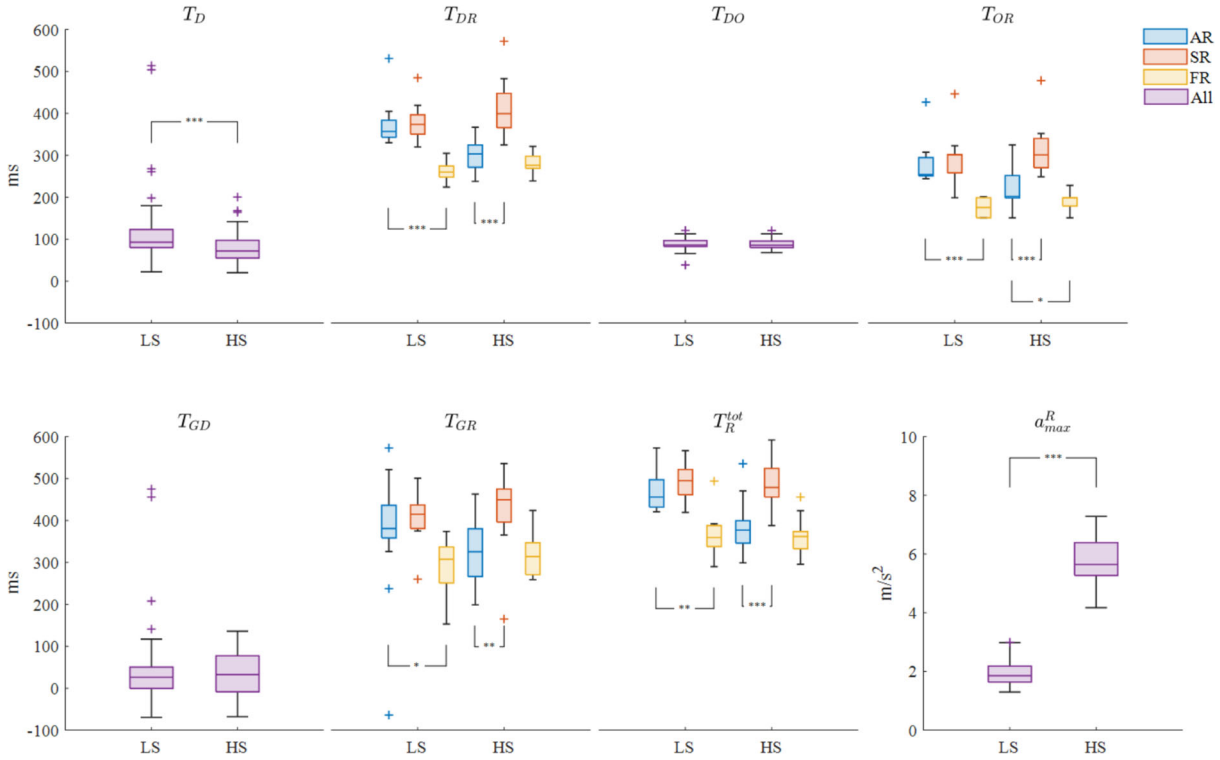

Fig. 4 Experimental results (objective metrics). Statistical significance is indicated with the following notation: significant * ($p < 0.05$), very significant ** ($p < 0.01$), highly significant *** ($p < 0.001$)

cuits to the signalling of the object release. It provides a measure of the ability of the proprioceptive filtering in achieving human-like handover reaction times for starting the object release. This is computed considering the onset of the contact between the receiver and the object;

- Time from grasp to release T_{GR}, as the time elapsed from the activation of both FSR circuits to the end of the object release. It compares release durations of the different policies (SR, FR and AR) with respect to timings measured in the human-to-human object handovers;
- Total time to release T_R^{tot}, as the time elapsed from the activation of one of the two FSR circuits to the end of the object release. It measures the total duration of the object release procedure, starting from the beginning of the physical handover phase.

4.2 Results

Fifteen healthy participants took part in the experiment (9 males and 6 females, aged 29 ± 7 years old).

Objective metrics are reported in Fig. 4. Median values are considered representative of the 6 experimental conditions (6 trials per condition) posed to participants. The hypothesis of normality is rejected for all distributions, according to the Kolmogorov-Smirnov test, thus statistical significance is assessed through the Wilcoxon rank sum test. $a_{\max}^R$ statistically differs ($p < 0.001$) between conditions LS and HS (respectively, 1.85 ± 0.54 and 5.64 ± 1.11 m/s^2). Noting that T_D, T_{GD}, and T_{DO} are not related to the release behaviour, a similar difference ($p < 0.001$) is also observed for T_D (93 ± 43 and 72 ± 43 ms), while not for T_{GD} (26 ± 51 and 33 ± 86 ms). No statistical difference is found for T_{DO} (86 ± 14 and 86 ± 15 ms).

For T_{DR}, T_{GR}, T_{OR} and T_R^{tot}, we compared the output metrics between different release behaviours, moreover, results are analysed separately for each of the two distinct levels of reaching speed. For the LS condition, the AR control law did not differ with respect to SR nor in terms of TDR, T_{GR}, T_{OR} or T_R^{tot}. Such a difference exists ($p < 0.001$, $p < 0.05$, $p < 0.001$, $p < 0.01$) instead between AR and the FR behaviour. The HS condition presents an opposite scenario, where differences exist if comparing AR with SR in terms of T_{DR}, T_{GR}, T_{OR} and T_R^{tot} ($p < 0.001$, $p < 0.01$, $p < 0.001$, $p < 0.001$). T_{OR} differs significantly ($p < 0.05$) also when comparing AR and FR.

Regarding the subjective metrics, Fig. 5 shows the relative probability of scores, measured from all trials. For the LS condition, a significant difference ($p < 0.05$) is observed when comparing scores given to the AR and SR behaviour, respectively. Such a difference does not exist when comparing AR and FR. In the HS condition, AR differs significantly

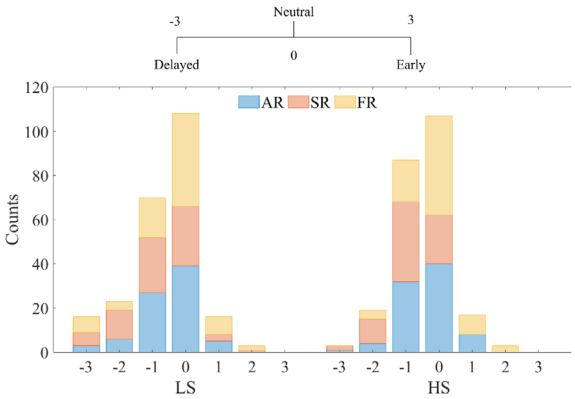

Fig. 5 Experimental results (subjective metrics). Cumulative count of coordination scores on a 7-point scale for both levels of reaching speed and with different release behaviours. Interactions rated with the null value are those rated the best in terms of coordination.

from the SR ($p < 0.001$) and from the FR ($p < 0.05$) behaviour.

5 Discussion and Conclusions

In this work, we investigated the application of the presented proprioceptive filtering technique in robot-to-human handover. Our effort was related to gaining the correct timing at the beginning of the object release in challenging conditions, for instance when the robotic giver must reach and coordinate with the human partner to successfully complete the collaborative action. We also investigated the efficiency of an adaptive (bio-inspired) control strategy for the object release, empowering our robotic agent with the capability to correlate its motor program with respect to the one selected by the human receiver.

The motion capture system was used to ease the data collection within the experiment which was strictly focused on contact sensing and on the physical part of the object handover. We believe that such a system could be actually replaced with any of the camera-based state-of-the-art methods which were effectively demonstrated for human pose estimation [29]. We also reiterate that FSRs on the test object are used in the scope of the present work only as assessment tool a posteriori for the performance of our proprioceptive filtering technique. They are not involved at any stage in the actual execution of robot-to-human handover demonstrated in our experiments.

The proposed method of signalling the object release, based on proprioceptive filtering, seems to ensure timings T_{GD} well aligned with reaction times observed in humans handing over objects (30 ± 47 and 26 ± 42 ms for slow and fast reaching respectively) [10]. Since any visual input is used by our agent to ensure predictive or anticipatory behaviour, the proprioceptive filtering technique has been proven to be sufficiently performing to detect the mild collision with the receiver, which arises at the beginning of the physical interaction phase of the handover action, independently from the speed of reaching movements.

For the HS condition, a slightly higher performance is shown in T_D. It should be noted that a mild collision between the two partners becomes more relevant in terms of the rate and entity of applied force/torques the higher the level of reaching speed/acceleration. Nonetheless, T_{GD} is not affected by the kinematics of the pre-handover phase, although in the fast condition, more variability is observed. This may be due to the greater level of coordination effort required of the participants when they had to rapidly grasp the test object.

The total duration T_R^{tot} of the physical interaction between the robotic giver and the human receiver is strongly affected by the T_{DO} lag, which seems to prevent the matching of durations observed in the present work with results from our previous study [10]. In the current scenario, considering the AR strategy, which correlates the release duration to visual cues observed in humans, median values of T_R^{tot} overcome the median release duration observed in humans of ∼130 ms (both for slow and fast reaching). Nonetheless, considering T_{GR} instead, the median values exceed by ∼50 and ∼80 ms. Release durations ranged between 300 and 500 ms, which are consistent to the findings in prior studies in humans [8].

In terms of subjective metrics, LS conditions do not highlight significant differences when comparing the AR strategy with the FR behaviour, almost half of the trials were rated with the null value, indicating good coordination of the robot with respect to the receiver intention, although the AR is more frequently perceived to produce delay in the handover action. For the HS conditions, the difference between AR and FR is stronger, while the first strategy keeps the same level of performance independently from the speed of the reaching movement, the latter is rated more positively. The SR behaviour is significantly perceived to produce excessively delayed coordination, both for LS and HS reaching movements.

In conclusion, the proposed methods were shown to be effective in gaining proper timing for the object release, while from subjective metrics we highlighted the importance of the release duration in the robot-to-human handover scenario, along with the applicability of a bio-inspired release control law. The AR has been proven to be highly relevant for HS reaching conditions, but also well suited for LS conditions, although it did not outperform a more simple fast feedforward release strategy.

We believe that the proprioceptive filtering method can be used without major adaptations by users differing for age and levels of experience with human-robot interactions since it considers the properties of the object rather than user inter-

action. Conversely, the proposed release control is derived from our earlier observations in human-to-human handovers [10], and it postulates a quadratic relationship between the peak acceleration of the receiver and the release duration by the robotic giver. Since the outcome of this controller affects the perception of the interaction, its optimal parameters may vary based on age or confidence in interacting with a robot. For instance, age is known to cause slight preference between slow and fast movement behaviors of articulated robot arms [30].

Although the handover performances of our robotic agent were generally well-perceived by users, we have not yet investigated this aspect in detail. Future research should focus on investigating if seamless handover enhances trust and fosters a greater willingness to collaborate with the robot over time.

Additionally, it would be highly valuable to expand the design of the release controller by incorporating additional parameters. This could lead to increased trust and contribute to a more satisfying interaction in the long run. In fact, different models with an increased number of hyperparameters could possibly lead to greater flexibility in terms of achieving higher levels of user personalization, which was recently proven to promote human operator confidence in the robot assistant, particularly for individuals with limited prior experience in robotics [31].

Further investigations may delve into the integration of Preference Learning (PL) techniques-along with the integration of suitable release policies-which are a very popular solution to tailor the interaction to each participant while also allowing for qualitative analysis of user preferences. In fact, PL both achieves the aim of investigating relevant hyperparameters to the human-robot interaction while also regulating their effect on the user experience [32].

Finally, future works, concerning the proprioceptive filtering technique, may lie on the adoption of state estimation techniques, to update online the estimate on the inertial set according to any new available kinematic and dynamic measurement during the reaching phase. As a result, the need for an ad-hoc estimation trajectory, prior to the actual reaching phase, might be obviated, increasing the portability of our method toward deployment in open world scenarios.

Author Contributions Not applicable.

Funding Open access funding provided by Scuola Superiore Sant'Anna within the CRUI-CARE Agreement. Marco Controzzi and Mattia Penzotti are supported by the European Commission under the Horizon 2020 framework program for Research and Innovation (project acronym: APRIL, project number: 870142).

Data Availibility Motion capture and robot sensory data can be made available upon reasonable request.

Code Availability Visit the project website https://penzottimattia.github.io/proprioceptive_release/.

Declarations

Conflict of interest The authors declare they have no conflict of interest.

Consent to Participate Participants enrolled on the study on a voluntary basis.

Consent for Publication Not applicable.

Ethical approval All procedures performed in the study involving human participants were in accordance with the ethical standards of the institutional committee and with the 1964 Helsinki declaration and its later amendments or comparable ethical standards. The study was approved by the local ethical committee of the Scuola Superiore Sant'Anna, Pisa, Italy (approval number 21/2022). Informed consent was obtained from the study participants.

References

1. Bommasani R, Hudson DA, Adeli E, Altman R, Arora S, Arx S, Bernstein MS, Bohg J, Bosselut A, Brunskill E, et al. (2021) On the opportunities and risks of foundation models. arXiv preprint arXiv:2108.07258
2. Selvaggio M, Cognetti M, Nikolaidis S, Ivaldi S, Siciliano B (2021) Autonomy in physical human-robot interaction: a brief survey. IEEE Robot Autom Lett 6(4):7989–7996
3. Ajoudani A, Zanchettin AM, Ivaldi S, Albu-Schäffer A, Kosuge K, Khatib O (2018) Progress and prospects of the human-robot collaboration. Auton Robot 42:957–975
4. Brose SW, Weber DJ, Salatin BA, Grindle GG, Wang H, Vazquez JJ, Cooper RA (2010) The role of assistive robotics in the lives of persons with disability. Am J Phys Med Rehabil 89(6):509–521
5. Haddadin S, Croft E (2016) Physical human–robot interaction. Springer handbook of robotics, 1835–1874
6. Cherubini A, Passama R, Crosnier A, Lasnier A, Fraisse P (2016) Collaborative manufacturing with physical human–robot interaction. Robot Comput Integr Manuf 40:1–13
7. Ortenzi V, Cosgun A, Pardi T, Chan WP, Croft E, Kulic D (2021) Object handovers: a review for robotics. IEEE Trans Robot 37(6):1855–1873. https://doi.org/10.1109/TRO.2021.3075365
8. Mason AH, MacKenzie CL (2005) Grip forces when passing an object to a partner. Exp Brain Res 163(2):173–187. https://doi.org/10.1007/s00221-004-2157-x
9. Cini F, Ortenzi V, Corke P, Controzzi M (2019) On the choice of grasp type and location when handing over an object. Sci Robot 4(27):9757

10. Controzzi M, Singh H, Cini F, Cecchini T, Wing A, Cipriani C (2018) Humans adjust their grip force when passing an object according to the observed speed of the partner's reaching out movement. Exp Brain Res 236(12):3363–3377. https://doi.org/10.1007/s00221-018-5381-5
11. Strabala K, Lee MK, Dragan A, Forlizzi J, Srinivasa SS, Cakmak M, Micelli V (2013) Toward seamless human–robot handovers. J Human–Robot Inter 2(1):112–132
12. Huber M, Radrich H, Wendt C, Rickert M, Knoll A, Brandt T, Glasauer S (2009) Evaluation of a novel biologically inspired trajectory generator in human-robot interaction. In: RO-MAN 2009-The 18th IEEE International Symposium on Robot and Human Interactive Communication, 639–644. IEEE
13. Prada M, Remazeilles A, Koene A, Endo S (2013) Dynamic movement primitives for human-robot interaction: comparison with human behavioral observation. In: 2013 IEEE/RSJ International Conference on Intelligent Robots and Systems, 1168–1175. IEEE
14. Ewerton M, Neumann G, Lioutikov R, Amor HB, Peters J, Maeda G (2015) Learning multiple collaborative tasks with a mixture of interaction primitives. In: 2015 IEEE International Conference on Robotics and Automation (ICRA), 1535–1542. IEEE
15. Maeda GJ, Neumann G, Ewerton M, Lioutikov R, Kroemer O, Peters J (2017) Probabilistic movement primitives for coordination of multiple human-robot collaborative tasks. Auton Robot 41:593–612
16. Iori F, Perovic G, Cini F, Mazzeo A, Falotico E, Controzzi M (2023) DMP-based reactive robot-to-human handover in perturbed scenarios. Int J Soc Robot 15(2):233–248
17. Ortenzi V, Cini F, Pardi T, Marturi N, Stolkin R, Corke P, Controzzi M (2020) The grasp strategy of a robot passer influences performance and quality of the robot–human object handover. Front Robot AI 7:542406
18. Moon A, Troniak DM, Gleeson B, Pan MK, Zheng M, Blumer BA, MacLean K, Croft EA (2014) Meet me where i'm gazing: how shared attention gaze affects human-robot handover timing. In: Proceedings of the 2014 ACM/IEEE International Conference on Human-robot Interaction, 334–341
19. Cini F, Banfi T, Ciuti G, Craighero L, Controzzi M (2021) The relevance of signal timing in human–robot collaborative manipulation. Sci Robot 6(58):1308
20. Chan WP, Parker CA, Loos HM, Croft EA (2012) Grip forces and load forces in handovers: implications for designing human-robot handover controllers. In: Proceedings of the Seventh Annual ACM/IEEE International Conference on Human-Robot Interaction, 9–16
21. Chan WP, Parker CA, Loos HM, Croft EA (2013) A human-inspired object handover controller. Int J Robot Res 32(8):971–983
22. Chan WP, Kumagai I, Nozawa S, Kakiuchi Y, Okada K, Inaba M (2014) Implementation of a Robot-human Object Handover Controller on a Compliant Underactuated Hand Using Joint Position Error Measurements for Grip Force and Load Force Estimations, 1190–1195 . https://doi.org/10.1109/ICRA.2014.6907004
23. Davari M-J, Hegedus M, Gupta K, Mehrandezh M (2019). Identifying multiple interaction events from tactile data during robot–human object transfer. https://doi.org/10.1109/RO-MAN46459.2019.8956306
24. Medina JR, Duvallet F, Karnam M, Billard A (2016) A Human-inspired Controller for Fluid Human-robot Handovers, 324–331 . https://doi.org/10.1109/HUMANOIDS.2016.7803296
25. Kubus D, Kröger T, Wahl FM (2007) On-line rigid object recognition and pose estimation based on inertial parameters, 1402–1408. https://doi.org/10.1109/IROS.2007.4399184
26. Bruyninckx H, De Schutter J (1996) Symbolic differentiation of the velocity mapping for a serial kinematic chain. Mech Mach Theor 31(2):135–148. https://doi.org/10.1016/0094-114X(95)00069-B
27. Magnani PL, Ruggeri G et al (1986) Meccanismi per Macchine Automatiche. Utet, Italy
28. Su Z, Hausman K, Chebotar Y, Molchanov A, Loeb GE, Sukhatme GS, Schaal S (2015) Force estimation and slip detection/classification for grip control using a biomimetic tactile sensor, 297–303 . https://doi.org/10.1109/HUMANOIDS.2015.7363558
29. Goyal G, Di Pietro F, Carissimi N, Glover A, Bartolozzi C (2023) Moveenet: online high-frequency human pose estimation with an event camera. In: Proceedings of the IEEE/CVF Conference on Computer Vision and Pattern Recognition, 4024–4033
30. Hostettler D (2024) The influence of demographic variation on the perception of industrial robot movements. arXiv preprint arXiv:2409.05049
31. Campagna G, Lagomarsino M, Lorenzini M, Chrysostomou D, Rehm M, Ajoudani A (2024) Promoting trust in industrial human–robot collaboration through preference-based optimization. IEEE Robot Autom Lett
32. Perovic G, Iori F, Mazzeo A, Controzzi M, Falotico E (2023) Adaptive robot-human handovers with preference learning. IEEE Robot Autom Lett

Marco Controzzi received his BSc and MSc in Mechanical Engineering in 2005 and 2008, respectively. In 2013, he received a PhD in Robotics and ICT form the Sant'Anna School of Advanced Studies and is currently Associate Professor of Bioengineering at the BioRobotics Institute of the Sant' Anna School of Advanced Studies. Research interests: design of artificial hands, human robot interaction, grasping and manipulation.

Mattia Penzotti received his BSc and MSc in Mechanical Engineering in 2019 and 2021, respectively. He is currently PhD Candidate at the BioRobotics Institute of the Sant'Anna School of Advanced Studies. Research interests: human robot interaction, robotic grasping and manipulation.